On the mechanical work absorbed on faults during earthquake ruptures

Massimo Cocco[1], Paul Spudich[2] and Elisa Tinti[1]

(1) Istituto Nazionale di Geofisica e Vulcanologia, Rome, Italy

(2) U.S.Geological Survey, Menlo Park, California, USA

November 07 2006
In press on the AGU Monograph on
Radiated Energy and the Physics of Earthquakes Faulting,
A. McGarr, R. Abercrombie, H. Kanamori and G. di Toro, Eds.

Abstract

In this paper we attempt to reconcile a theoretical understanding of the earthquake energy balance with current geologic understanding of fault zones, with seismological estimates of fracture energy on faults, and with geological measurements of surface energy in fault gouges. In particular, we discuss the mechanical work absorbed on the fault plane during the propagation of a dynamic earthquake rupture. We show that, for realistic fault zone models, all the mechanical work is converted in frictional work defined as the irreversible work against frictional stresses. We note that the γ_{eff} of Kostrov and Das (1988) is zero for cracks lacking stress singularities, and thus does not contribute to the work done on real faults. Fault shear tractions and slip velocities inferred seismologically are phenomenological variables at the macroscopic scale. We define the macroscopic frictional work and we discuss how it is partitioned into surface energy and heat (the latter includes real heat as well as plastic deformation and the radiation damping of Kostrov and Das). Tinti et al. (2005) defined and measured breakdown work for recent earthquakes, which is the excess of work over some minimum stress level associated with the dynamic fault weakening. The comparison between geologic measurements of surface energy and breakdown work revealed that 1-10% of breakdown work went into the creation of fresh fracture surfaces (surface energy) in large earthquakes, and the remainder went into heat. We also point out that in a realistic fault zone model the transition between heat and surface energy can lie anywhere below the slip weakening curve.

1. INTRODUCTION

Fracture mechanics has long been considered a reference framework for interpreting dynamic earthquake ruptures for both shear and tensile cracks. Linear elastic fracture mechanics (LEFM) has its roots in the Griffith energy balance theory (Parton and Morozov, 1974; Scholz, 1990). Although it has always been clear that earthquakes in natural faults are much more complex, this approach has often been used to identify and describe the different physical terms defining the energy balance and the mechanical work required to allow dynamic rupture propagation. The aims of this paper, consistent with the goals of the Monograph, are to discuss the mechanical work absorbed on the fault plane during the propagation of a dynamic earthquake rupture, its partitioning into surface energy and heat, and its scaling with earthquake moment. To these goals it is helpful to review the basic concepts which lead to the definition of the main physical factors relevant to this problem. We start by discussing several distinct fault zone models: a static Griffith crack, an elastic-brittle fracture (i.e., an Irwin crack), a slip-weakening fault zone model (Ida, 1972; Andrews, 1976-a and -b), and a more realistic fault model accounting for the structure and thickness of natural faults (see Sibson, 2003 and references therein). We will not consider the earthquake nucleation problem and we will focus our attention on the dynamics and the energy required to sustain earthquake propagation.

Several recent studies make available seismological (e.g. Rice et al. 2005; Tinti et al. 2005) and geological (Chester et al., 2005; Wilson et al., 2005) measurements of energies absorbed on faults. In this study we reconcile these measurements with each other and with theory; we clarify the differences between theoretical terms like fracture energy and observational quantities like surface energy. For example, different authors use the term fracture energy to mean different quantities. Fukuyama (2005) defines fracture energy to be equal to the Kostrov term appearing in the definition of radiated seismic energy; other authors implicitly associate fracture energy with surface energy. Also the term friction is used with different meanings. Therefore, we introduce self-consistent definitions of these terms, which can be applied to seismological and geological observation of absorbed energy as well as to results from laboratory experiments on rock mechanics.

The fracture energy is one of the key ingredients required to describe the energy flux per unit area at the crack-tip. It is the energy absorbed by the crack that controls rupture speed. The dynamic energy release rate (see Freund, 1979; Li, 1987), which is related to the flux of

elastic energy into the vicinity of the crack tip, decreases with increasing rupture velocity. In classic fracture mechanics, rupture velocity is determined by matching energy release rate to fracture energy. The application of these concepts to a slip-weakening model leads to the identification of fracture energy on the shear traction evolution curve (see Palmer and Rice, 1973; Li, 1987). In a slip-weakening stress-slip plot the fracture energy (G) is the area under the curve above the residual stress level (as shown in Figure 1). This parameter is relevant to the classical fracture criterion; it determines rupture velocity and it has been estimated both through laboratory experiments (see Li, 1987, and references therein) and seismological investigations (see Rice et al., 2005; Tinti et al., 2005, and references therein).

In this paper we discuss the energy absorbed on the fault plane and the mechanical work. We define the frictional work as the irreversible part of mechanical work, which is the part of the mechanical work that does not go into elastic strain energy and kinetic energy. Because the measurable physical quantities characterizing dynamic fault weakening (shear stress, slip, slip rate) must be considered macroscopic quantities (Ohnaka, 2003), we define the macroscopic frictional work to be the contribution to the energy absorbed on the fault plane for a realistic fault zone model. It is important to emphasize that both laboratory and seismological estimates of shear traction evolution and slip time history are macroscopic because stresses and displacements on natural or experimental faults can only be inferred with limited accuracy from remote observations. They differ from microscopic mathematical models (such as the classic Griffith or Irwin crack models) in which stress and displacement can be determined exactly at any point. These fracture mechanical models should not be considered as proxies for earthquake ruptures on natural faults. An important implication of these findings is that fracture energy contains not just surface energy but also energy dissipated by other processes.

2. FAULT ZONE MODELS

2.1. Classical Fracture Mechanical Models.

We start describing the simplest and unrealistic fault zone model represented by a mode I (opening) Griffith crack (Griffith, 1920; Li, 1987, among many others) consisting of a fracture surface which is cohesionless behind the crack tip and which has a stress concentration (singularity) at its tip. In the context of a shear crack the term “cohesionless” means “frictionless” (that is, zero friction). This approach characterizes the fracture as a

balance between the available energy G to drive the crack and the energy absorbed by the inelastic processes at the crack-tip. Another well-known approach relies on the work of Irwin (1960), who characterized the stress field at the crack tip in terms of a stress intensity factor K_i. Both these approaches can be formulated in terms of fracture criteria ($K_i = K_{ic}$ and $G = G_c$) that are perfectly consistent in a linear elastic body. According to LEFM the condition for crack propagation (for a plane stress configuration) is met when

$$G_c = \frac{K_c^2}{E} = 2\gamma \tag{1}$$

where G_c is the fracture energy, K_c is the critical stress intensity factor, E is the effective Young modulus and γ is the specific surface energy (see Scholz, 1990 and references therein). This yields the definition of fracture energy as the available energy to drive the crack propagation, which is absorbed by inelastic processes at the crack-tip. According to its definition, in a Griffith crack all the fracture energy is surface energy (as clearly stated in equation 1).

When more realistic crack tip processes are considered, energy sinks in addition to surface energy contribute to fracture energy. Scholz (1990) points out that deformation near a crack tip occurs as complex microcracking distributed over the region known as the brittle process zone. As the crack advances, at some distance behind the tip of the process zone the microcracks link to form a macroscopic fracture. In such a model all the dissipation (distributed cracking, plastic flow …) occurs within the process zone. Thus, because the crack tip is surrounded by the process zone (where LEFM is not applicable, see Li, 1987), the specific surface energy (γ) has to be defined as a macroscopic parameter. For this reason Irwin (1960) proposed the use of the effective surface energy γ_{eff} as a macroscopic contribution of the total energy absorbed during the fracture development within the process zone at the crack-tip. Thus, according to Irwin, the fracture energy is given by $G_c = 2\gamma_{eff}$. The quantity γ_{eff} is a lumped parameter that includes all dissipation within the crack-tip region (Scholz, 1990). This implies that, although it is called effective surface energy by analogy with equation (1), it includes not only surface energy but also other dissipative mechanisms such as heat (Kostrov and Das, 1988, hereinafter KD88). In both a Griffith and a Irwin-Orowan crack the stress has a singularity at the crack tip.

In this paper we will use the term *friction* to mean the total instantaneous dynamic traction ($\tau_i = \sigma_{ij} n_j$) acting on the fault plane (where σ_{ij} is the current stress and n_j is the unit vector normal to that plane).

2.2. The Breakdown Zone Model.

The assumption that a shear crack is frictionless behind its tip is unrealistic and does not allow a description of faulting (Scholz, 1990). The concept of "breakdown," by which we mean a finite force between the two crack faces which varies continuously from an initial level to some minimum level as the faces progressively slip or open, has been introduced by Barenblatt (1959) and Ida (1972) for tensile and shear cracks, respectively, to avoid infinitely large stress concentrations on the fracture plane. In this paper we shall use the term "breakdown zone" to mean the region of a locally 2D crack between the crack tip and the point having minimum stress behind the crack tip. Sometimes this zone is called the "cohesive zone", but in this paper we avoid the use of the mode I term cohesion for shear cracks. Our use of the term breakdown is consistent with the definition for real rocks given by Ohnaka (1996). One form of breakdown zone model, the linear slip weakening model (Ida, 1972; Palmer and Rice, 1973; Andrews, 1976-a, -b), has been widely adopted in the literature. According to this model (Figure 1) slip (Δu) starts at a point on a fault when the local shear stress reaches a yield upper level (τ_y), the shear stress required to sustain slip is reduced to a residual level (τ_f) as the slip is increased to a critical amount (D_c) and further slip occurs with shear stress at the residual level. The analytical form of this constitutive law is given by the following expression (Andrews, 1976a):

$$\tau = \begin{cases} \tau_y - (\tau_y - \tau_f)\Delta u / D_c, \rightarrow \Delta u < D_c \\ \tau_f, \rightarrow \Delta u > D_c \end{cases}$$

This model involves frictional sliding and therefore mechanical work done against frictional stress is irreversible. It is lost to the mechanical system and goes into heat or other loss mechanisms, as we will discuss in the following. Frictional sliding occurs everywhere behind the crack tip; frictional stress in a finite region behind the crack-tip is larger than residual stress.

2.3. Geological Fault Zone Model.

Field observations reveal that natural fault zones are characterized by slip localization within a complex structure (see Sibson, 2003, and references therein). Slip occurs on a principal slipping zone typically located in an ultracataclastic fault core, which is surrounded by a damage zone. The main implication of these observations is that faults have a finite thickness (although sometimes very narrow, ≈ mm) and are filled by gouge and wear materials produced during faulting. The temperature changes during coseismic slip episodes depend on the thickness of the slipping zone (see Andrews, 2002; Fialko, 2004; Bizzarri and Cocco, 2006-a, -b and references therein); melting can occur (see Sibson, 1973; Di Toro et al., 2005) on a slipping fault, but there is no observational agreement on the prevalence of melting. If we account for such a complex fault zone, the damage zone should not be considered as an elastic brittle medium, but as a poro-elastic and/or plastic medium. In such a fault model the available mechanical energy can be dissipated in many different ways and the physical meaning of surface energy and frictional work should be defined carefully. We aim to discuss these issues in this paper.

One significant consequence of considering this complex fault structure concerns the definition of the main observable physical quantities characterizing the rupture process. In such a complex fault zone the shear traction used to describe dynamic fault weakening cannot be considered to be the shear stress acting on individual gouge fragments or microcracks within the slipping zone (Ohnaka, 2003). Therefore, the shear stress, the slip and the slip velocity should be considered in a macroscopic sense; the dynamic traction is the stress acting on the walls of the fault zone having a finite thickness. Similarly, the slip (or slip velocity) is the relative displacement (or rate) between both walls of fault zone of finite thickness. This definition should be applied to seismological estimates of dynamic shear traction, like those obtained by Ide and Takeo (1997), Day et al. (1998), and Tinti et al. (2005). Even on the laboratory scale Ohnaka (2003) suggests that the shear stress, slip and slip velocity used in the constitutive formulation derived from laboratory experiments should be considered as macroscopic variables, i.e. macroscopic averages of complex processes (asperity fractures, gouge formation and evolution, etc…) occurring within the slipping zone. In this context, fault friction on all scales but the atomistic should be considered in a macroscopic sense or as a phenomenological description of complex processes occurring within the fault core. This issue is of particular interest for this study because shear traction evolution characterizes

dynamic fault weakening (Rice and Cocco, 2006). From the shear traction evolution the energy absorbed on the fault plane and the fracture energy can be calculated.

Tinti et al. (2005) performed such calculations on the seismological scale and defined a quantity "breakdown work" (W_b) inferred for real earthquakes, which is related to fracture energy but not necessarily identical, as we will discuss later in this study. Breakdown work contains a mixture of heat and surface energy (energy that goes into fracture and gouge formation) as schematically illustrated in Figure 2.

3. THE MECHANICAL WORK ON THE FAULT PLANE

In order to define the different terms contributing to the energy flux on the fault plane, it is useful to start from the earthquake energy balance. We follow the classic formulation of the earthquake energy balance proposed by KD88 and we write it in terms of an energy conservation law for a body containing a propagating crack as follows:

$$\dot{A} - \dot{U} - \dot{K} = -\dot{Q} \tag{2}$$

where $\dot{A}$ is the rate of work done by external forces, $\dot{U}$ is the rate of change of internal energy, $\dot{K}$ is the rate of change of kinetic energy and $\dot{Q}$ has been defined as the heat power (the rate of irreversible work done by stress within the body). The last term contains all the energy dissipated during dynamic fracture, such as surface energy, heat and energy radiated out from the crack-tip as high-frequency (near-field) stress waves (see KD88; Rice et al., 2005). The analytical expressions of the four terms appearing in equation (2) are described by Kostrov and Das (KD88, equations from 2.2.2 to 2.2.4). In the short duration of dynamic fault weakening, the surface energy should be associated with irreversible processes included in the dissipative terms. We will discuss later in this section some of the different dissipative processes which may be included in $\dot{Q}$ depending on the fault zone model adopted. It is important to point out that the sum on the left side of equation (2) can be considered to be the rate of mechanical energy (see Freund, 1979).

KD88 derive the terms in equation (2) for three different integration domains. In the simplest case in which the volume V does not contain the fracture surface Σ, the solution is the local form of the energy conservation law for a continuous medium (see KD88, eq.2.2.9):

$$\rho\dot{e} = \sigma_{ij}\dot{\varepsilon}_{ij} - q_{i,i}$$

where $\rho\dot{e}$ is the rate of internal energy density, σ_{ij} is the instantaneous stress, $\dot{\varepsilon}_{ij}$ is the strain rate and $q_{i,i}$ is the divergence of the heat flux vector q_i.

The second solution for a volume V containing the crack surface, but not its tip, is most relevant to our study. KD88 (eq. 2.2.16) derived the following relation between mechanical work, surface energy, and heat generation on a specific point of a fault surface not including the crack edge:

$$\tau_i \Delta\dot{u}_i = 2\dot{\gamma} + \Delta q \tag{3}$$

where τ_i (= g_i in KD88) is the traction and $\Delta\dot{u}_i$ (= $\dot{a}_i$ in KD88) is the slip velocity on the fault plane Σ; γ is the specific internal surface energy and $\dot{\gamma}$ is the surface energy rate, Δq is the difference in heat flux per unit area across the fault plane (i.e. the flux generated on the fault). It is important to point out that the specific surface energy appearing in (3) (actually its rate $\dot{\gamma}$) does not correspond to the Griffith surface energy defined in (1). As discussed in the previous section, only for a static Griffith crack is all the fracture energy surface energy. However, we cannot consider Griffith cracks to be fracture mechanical models for earthquakes. Equation (3) is applicable to fault zone models with breakdown zones. As we will discuss in the next section, it allows the definition of the frictional work on the slipping region of the fault plane. Equation (3) states that the mechanical work on the fault plane is partly spent in the change of surface energy and partly released into the medium as heat. This implies that in a macroscopic description the mechanical work, or the energy supplied by the environment, is described by the work of tractions acting on the fault surface. Kostrov (1974) and KD88 (p. 65) explain that the term Δq contains not only the actual heat but also "radiation loss," energy radiated from the crack as high frequency stress waves dissipated near the fault.

Finally, KD88 provide a solution of equation (2) for a volume V intersecting the fault surface and containing its edge (i.e., the crack-tip). This solution (equations 2.3.1 and 2.3.2, p.68) yields the definition of the effective surface energy γ_{eff}:

$$\gamma_{eff} = \gamma - \frac{1}{2v_r}\lim_{\xi\to 0}\int_{\ell}\left[q_i + v_i\int_0^t q_{j,j}\,dt\right]n_i\,dl = -\frac{1}{2v_r}\lim_{\xi\to 0}\int_{\ell}\left\{\sigma_{ij}\dot{u}_j + v_i\left[\int_0^t \sigma_{jk}\dot{\varepsilon}_{jk}\,dt + \frac{1}{2}\rho\dot{u}_j\dot{u}_j\right]\right\}n_i\,d\ell \tag{4}$$

where $q_{j,j}$ is the divergence of the heat flux vector q_i, v_r is the rupture velocity ($v_r = \sqrt{v_i v_i}$), ξ is the diameter of an infinitesimal tube surrounding the crack tip, n_i are the components of the normal to the tube surface, $\dot{u}_i$ are the components of particle velocity and l is the integration

path around the crack-tip. This relation allows the definition of the Irwin's effective surface energy and it states analytically that at the crack tip the mechanical work is partly converted into surface energy (γ) and partly dissipated in the form of heat. It also shows that the flux of energy to the crack tip depends on rupture velocity, not only due to the explicit dependence in (4), but also because stress and slip velocity on the tube depend on rupture speed.

Equations (3) and (4) allow a physical description of some of the distinct fault zone models discussed in previous section. In fact, for either a Griffith or an Irwin-Orowan crack, which are frictionless on the fault plane, all the mechanical work is absorbed at the crack-tip, where the stress is singular. For an Irwin crack this allows the definition of the macroscopic fracture energy as $G_c = 2\gamma_{eff}$. It is important to note that in this configuration (which does not apply to the static Griffith crack, which we will not consider further) fracture energy does not correspond strictly to surface energy, but it also includes other dissipative processes. On the contrary, for those crack models (such as the breakdown zone model) in which the stress is not singular at the crack tip, the effective surface energy is zero, $\gamma_{eff} = 0$ (p.70 of KD88; Rudnicki and Freund, 1981; Fukuyama, 2005). This is evident from equation (4) which shows that as the tube radius goes to zero, γ_{eff} goes to zero if the integrand is not singular. We will discuss this issue further below.

4. THE ENERGY FLUX ON THE FAULT PLANE

In this section we focus on the energy flux on the fault and we provide a definition of the frictional work. We start discussing the relationship between radiated seismic energy, mechanical work on the fault and elastic potential energy. In particular, we derive a relation between surface energy, frictional work and the so-called Kostrov term. The energy radiated through a surface S_o completely enclosing a crack was given by KD88 (their eq. 4.4.21, with an incorrect minus sign corrected below) as:

$$E_r = \frac{1}{2}\iint_{\Sigma_0}(\sigma_{ij}^0 + \sigma_{ij}^1)n_j \Delta u_i^1 dS - \iint_{\Sigma_0} 2\gamma_{eff} dS - \int_{t_0}^{t_1} dt \iint_{\Sigma(t)} \sigma_{ij} n_j \Delta \dot{u}_i dS + \frac{1}{2}\iint_{S_o}(\sigma_{ij}^0 - \sigma_{ij}^1)n_j u_i^1 dS \qquad (5)$$

where Δu_i^1 is the final slip; σ_{ij}^0 and σ_{ij}^1 are the initial and final stress values, respectively; n_j is the normal unit vector to the fault surface Σ_0; t_0 and t_1 are two reference times before and after the earthquake, respectively, and $\Sigma(t)$ is the ruptured fault surface at time t. Although in this paper we focus on the work done on the fault plane (we will call it ΔE_Σ, as defined

below), it is important to discuss the different terms appearing in the right side of equation (5). The first term is the elastic strain energy on the fault, which does not depend on the instantaneous stress σ_{ij}, but only on the initial and final stress values; the last term is the contribution from static displacements on S_o to the energy flux through ΔE_{So} (see also Rivera and Kanamori, 2005). In particular, we focus here on the second and third terms, which allow the definition of the energy absorbed on the fault plane:

$$\Delta E_{\Sigma} = \int_{t_0}^{t_1} dt \iint_{\Sigma(t)} \tau_i \Delta \dot{u}_i dS + \iint_{\Sigma_0} 2\gamma_{eff} dS , \qquad (6)$$

containing the instantaneous shear traction, $\tau_i = \sigma_{ij} n_j$. The integrand of the first term is given by equation (3), while that of the second term by (4). Very often the second term is called the fracture energy, but as we will show in the following this definition is not appropriate for realistic fault zone models. According to equation (6) and in agreement with KD88 and Rivera and Kanamori (2005) we define the frictional work as:

$$U_f = \int_{t_0}^{t_1} \dot{U}_f dt = \int_{t_0}^{t_1} dt \iint_{\Sigma(t)} \sigma_{ij} n_j \Delta \dot{u}_i dS = \int_{t_0}^{t_1} dt \iint_{\Sigma(t)} \tau_i \Delta \dot{u}_i dS . \qquad 7)$$

Frictional work is irreversible or non-elastic work, because slip is non-elastic strain. We point out that the quantities defined in (5), (6) and (7) are global quantities calculated for the whole fault plane. If now S_o is taken far away from the fault the last term in equation (5) vanishes and the radiated energy becomes (KD88 4.4.23)

$$E_r = \frac{1}{2} \iint_{\Sigma_0} (\sigma_{ij}^1 - \sigma_{ij}^o) n_j \Delta u_i^1 dS - \iint_{\Sigma_0} 2\gamma_{eff} dS - \int_{t_0}^{t_1} dt \iint_{\Sigma(t)} (\sigma_{ij} - \sigma_{ij}^o) n_j \Delta \dot{u}_i dS . \qquad (8)$$

This equation has also been presented by Rivera and Kanamori (2005, eq.12) and Fukuyama (2005, eq.2). Following KD88 (eq. 4.4.24; see also Rivera and Kanamori, 2005) an alternative expression of (8) can be obtained after integrating the last term by parts, yielding

$$E_r = \frac{1}{2} \iint_{\Sigma_0} (\sigma_{ij}^o - \sigma_{ij}^1) n_j \Delta u_i^1 dS - \iint_{\Sigma_0} 2\gamma_{eff} dS + \int_{t_0}^{t_1} dt \iint_{\Sigma(t)} \dot{\sigma}_{ij} n_j \Delta u_i dS . \qquad (9)$$

Equation (9) is the same as equation (2.26) in Kostrov (1974). The main difference between equations (5) and (9) concerns the expression for the frictional work. In (5) and (7) the frictional work depends on the slip velocity evolution, while in (9) it is written as a function of the temporal derivative of the instantaneous stress. The last term in the right side of (9) is sometime called the Kostrov term. Because of its derivation, the Kostrov term has the

physical meaning of frictional work (it is the frictional work plus a constant depending on the final stress and slip values). Kostrov (1974) points out that equation (9) relates radiated energy to the static stress changes (first term) and to the fracture propagation (last term); he says: "*the last term will not always vanish and may be responsible for large part of the seismic energy. In any case the short wavelength part of the energy, responsible for the destructive action of the earthquake, must be concentrated mostly in this term. .... We investigate the conversion of energy by friction related to the break. Part of this energy is converted directly into heat: however, part of the loss during the slipping of rough surfaces is short-wave radiation. This part should be called radiative loss, and the corresponding contribution to the slip resistance could be called radiative friction*".

Equation (9) is the same as equation (5) in Fukuyama (2005). In that paper he defined the Kostrov term (i.e., the last term appearing in 9) as the fracture energy, although in that equation the effective surface energy γ_{eff} is still present. We will show in the next section that the equivalence of the Kostrov term with fracture energy is correct only for a classic slip weakening model in which the final stress is equal to the residual stress value (that is, with no overshoot or undershoot, see McGarr, 1994 for definition) as shown in Figure 1.

In the previous section we have shown that in a breakdown zone fault model the effective surface energy is zero ($\gamma_{eff} = 0$). Therefore, in this mechanical configuration the energy absorbed on the fault plane defined in equation (6) should be defined solely by the frictional work. In such a fault zone model the frictional work (defined by equations 3) expresses the mechanical work absorbed in a specific fault position (ζ_o) after this point starts to slip.

If we now wish to apply these considerations to a natural fault zone with finite thickness, as described in the previous section, we have to consider the main physical parameters (stress, slip and slip velocity) as macroscopic parameters. This means that we consider these quantities characterizing dynamic fault weakening as "equivalent" physical quantities acting on the walls of fault zone of finite thickness and we represent them as tractions or slip or slip velocity on a "virtual mathematical" fault plane at the macroscopic scale. In this framework, equation (3) is still valid and allows the definition of the macroscopic frictional work, while equation (7) defines the global contribution for the whole fault. Because in such a macroscopic fault zone model we still assume that the stress is finite at the crack tip, we still assume that $\gamma_{eff} = 0$. In the following we will always refer to these

physical parameters as macroscopic parameters. More generally frictional work should also account for the energy loss outside the slipping zone (see Andrews, 2005). The definition of the macroscopic frictional work allows us to describe the inelastic dissipation occurring during earthquakes and faulting and therefore permits us to specify the different contributions to the heat flux rate $\dot{Q}$ included in equation (2). The mechanical work is converted into frictional work (irreversible work), that is partitioned in surface energy, heat (including the radiation loss) and plastic deformation within the fault zone. Geologic studies of fault zones suggest that plastic deformation, in the form of mineral grain deformations, is negligible with respect to fault core surface energy and heat (Chester et al.,1993: Chester et al., 2005). Andrews (2005) has pointed out that the energy loss in a fault damage zone contributes to the fracture energy that determines rupture velocity in an earthquake. His calculations provide evidence that fracture energy should not be considered a constitutive property.

5. THE MACROSCOPIC FRICTIONAL WORK

As we have seen above, for a non-singular crack model as well as for a natural fault zone $\gamma_{eff} = 0$, so the frictional work contains all the energy dissipated on the fault during sliding.

By integrating equation (3) in time we get a definition of the macroscopic frictional work at a specific point on the fault plane. A subsequent integration on the whole fault plane yields the global macroscopic frictional work definition:

$$U_f = \iint_{\Sigma_0} dS \int_{t_r(\xi)}^{t_m(\xi)} \tau_i \Delta\dot{u}_i dt = \iint_{\Sigma_0} dS \int_0^{\Delta u_i^1} \sigma_{ij} n_j d(\Delta u_i) \tag{10}$$

where Δu_i^1 is the final slip value, $t_m(\xi)$ is the local healing time and $t_r(\xi)$ is the rupture time. It is important to note that slip velocity at any point on the fault is different from zero only in a time interval comprised between $t_r(\xi)$ and $t_m(\xi)$, when the slip varies from 0 to Δu_i^1. Equation (10) is equivalent to equation (7) because the integrand ($\tau_i \Delta\dot{u}_i$) does not contain any singularity and stress changes are considered up to the end of slip (when slip velocity becomes zero). This implies that stress evolution following the healing of slip ($t > t_m(\xi)$) does not contribute to the frictional work. It is useful to explicitly write the global (i.e., for the whole fault plane) and local (i.e., for a single fault position) expressions of frictional work:

$$U_f = \iint_{\Sigma_0} \Im_f dS = \iint_{\Sigma_0} dS \int_0^{\Delta u_i^1} \tau_i d(\Delta u_i) \tag{11a}$$

$$\Im_f = \int_{t_r}^{t_m} \sigma_{ij} n_j \Delta \dot{u}_i dt = \int_{t_r}^{t_m} \tau_i \Delta \dot{u}_i dt = \int_0^{\Delta u_i^1} \tau_i d(\Delta u_i) \tag{11b}$$

where $\Im_f$ is the frictional work density (work per unit area).

As discussed above, one important implication arising from our calculations is that the effective surface energy γ_{eff} is not included in the area below the shear traction in a traction versus slip plot. If the stress is not singular at the crack tip, $\gamma_{eff} = 0$ and it should not be considered in the analytical expression used to compute radiated energy (as equations 5 or 9). Moreover, equations (11a) and (11b) define the frictional work for the whole fault (global) and for a specific fault position (local). In order to identify the energy flux on the fault surface, it is important to first discuss the partitioning of the energy density at a single specific point on the fault plane. The evaluation of the frictional work at a specific point on the fault plane is not a common procedure and relies on knowledge of the dynamic traction evolution.

It is important to discuss the difference between the macroscopic frictional work and the Kostrov term, which we write as:

$$\int_{t_0}^{t_1} dt \iint_{\Sigma(t)} \dot{\sigma}_{ij} n_j \Delta u_i dS = \iint_{\Sigma_0} dS \int_0^{t_m} \dot{\sigma}_{ij} n_j \Delta u_i dt \, .$$

We now consider only the local values of these quantities in a specific fault position and we write (Eiichi Fukuyama written communication, 2005):

$$\int_0^{t_m} \dot{\sigma}_{ij} n_j \Delta u_i dt = \int_0^{t_m} \dot{\tau}_i \Delta u_i dt = \tau_i^1 \Delta u_i^1 - \int_0^{t_m} \tau_i \Delta \dot{u}_i dt = -\int_0^{\Delta u_i^1} \left(\tau_i - \tau_i^1 \right) d\Delta u_i \tag{12}$$

This equation clearly shows that, if the final stress τ_i^1 is equal to the residual stress τ_f and the latter is constant and equal to the minimum stress (as in a slip weakening model, as shown in Figure 1), the Kostrov term corresponds to the fracture energy G (as suggested by Fukuyama, 2005). However, in a more general case in which the final stress does not correspond to the minimum or residual value (as that drawn in Figure 2 typical of an undershoot model) the Kostrov term integrates the positive and negative oscillations of total dynamic traction as schematically drawn in Figure 3 (see also Kanamori and Rivera, this volume). Moreover, the fact that for the slip weakening model shown in Figure 1 the fracture energy G in equation (9) is included in the Kostrov term is a further corroboration that the

effective surface energy γ_{eff} does not lie within the traction versus slip curve, and it should be neglected in any other fault zone model with non-singular stresses.

Tinti et al. (2005) have defined an alternative measure of work to be used instead of fracture energy (G) to characterize traction evolution curves from kinematic models of real earthquake ruptures. These authors defined the excess of work over the traction level having minimum magnitude ($\vec{\tau}_{\min}$) achieved during slip, which they called breakdown work (W_b):

$$W_b = \int_0^{T_b} \left(\vec{\tau}(t) - \vec{\tau}_{\min}\right) \cdot \Delta\dot{\vec{u}}(t) dt \tag{13a}$$

where $\Delta\dot{\vec{u}}(t)$ is slip velocity and $\vec{\tau}(t)$ is shear traction; T_b is the time at which minimum traction $\vec{\tau}_{\min}$ is reached at the point (i.e., the breakdown time). W_b is an energy density (J/m^2), but it is called breakdown work for simplicity. It is equivalent to "seismological" fracture energy (G) in simple models without overshoot or undershoot (Figure 1). Tinti et al. (2005) have defined the excess work W_e as the sum of breakdown work and restrengthening work (W_b and W_r, respectively), as schematically shown in Figure 2, where restrengthening work is defined as

$$W_r = \int_{T_b}^{t_m} \left(\vec{\tau}(t) - \vec{\tau}_{\min}\right) \cdot \Delta\dot{\vec{u}}(t) dt \tag{13b}$$

where t_m is the healing time of slip at the point; W_r is also an energy density. We will discuss later in this study the presence of restrengthening work in traction evolution curves and we focus now on the breakdown work. The reason why Tinti et al. (2005) proposed use of the term breakdown work W_b is relatively simple: the light-gray shaded area arbitrarily drawn in Figure 2 and computed through equation (13-a) is the energy density (or work) associated with the breakdown phase (i.e., the evolution of traction from the initial level to the minimum value) and it is used to allow the rupture to advance at a determined rupture velocity.

For real earthquakes, breakdown work probably contains a mixture of heat and surface energy (energy that goes into fracture and gouge formation) as schematically illustrated in Figure 2. In other words, it is likely that the boundary between heat and surface energy does not lie along a horizontal line at $\vec{\tau}_{\min}$ (as often depicted, see Figure 1 and Kanamori and Heaton, 2000, and references therein). This is perfectly consistent with our calculations presented above. The integral over the fault surface of breakdown work W_b allows the definition of the breakdown energy E_b, which is a global quantity measuring the

contribution of the whole fault. It is important to emphasize that the traction behavior illustrated in Figure 2 is a schematic diagram, not a real calculation or measurement. Tinti et al. (2005) have inferred the shear traction evolutions from kinematic rupture models of several recent earthquakes. We will present some examples of these calculations in section 7.

6. LABORATORY ESTIMATES OF FRACTURE ENERGY

Laboratory experiments have been conducted during last decades to provide insights on the mechanics of earthquake rupture as well as to estimate the main parameters directly related to the physics of rupture process (as fracture energy, friction coefficient, stress drop, critical slip-weakening distance) and useful scaling relations. The experiments have been done either with intact rocks (Kato et al. 2003; Ohnaka et al. 1997; Wong, 1982; Moore and Lockner, 1995; among many others) or with pre-existing surfaces (Okubo and Dieterich 1984; Rummel et al. 1978; Lockner and Okubo 1983; Shimamoto and Tsutsumi, 1994. among many others) with bi- and tri-axial apparatus. The major limitation of laboratory experiments consists in the difficulty of reproducing the temperature-pressure conditions at seismogenic depth. In fact, the constitutive properties of fault zones greatly depend on these ambient conditions. Results from laboratory experiments provide fracture energy estimates ranging between 10^3 and 10^5 J/m^2. They are smaller than seismological estimates (10^6 - 10^7 J/m^2; see Rice et al., 2005 and references therein). This difference might depend on the higher normal stress at ambient conditions at seismogenic depth, higher final slip and D_c values for natural faults, differing amounts of gouge production, as well as differences in roughness of fault surfaces. All these factors might account for the inferred gap between laboratory and seismological estimates of fracture energy or breakdown work (McGarr et al., 2004).

Because in this study we are interested in discussing the partitioning between surface energy and heat, we focus now on the few laboratory experiments that evaluated heat during dynamic failure episodes. Lockner and Okubo (1983) computed the energy budgets of stick-slip events in a large biaxially–loaded sample for a saw-cut granite [precut fault area was 0.8 m^2; the inferred seismic moment ranges between 1· and 3·10^6 N·m]. They measured the temperature on their rock sample and inferred the heat generated by the slip events. They found low values (0.04 - 0.08) of efficiency (seismic energy over strain energy) and they suggest that "*most of the energy released during seismic slip is consumed in overcoming frictional resistance and manifests itself as heat*." They assumed that traction evolution

follows that depicted in Figure 1 and concluded that almost all the work was heat and fracture energy was negligible. In fact, they measured the generated heat to be 1.04 times the product of slip and residual stress, meaning that the boundary between heat and surface energy in their experiment could be similar to that in Figure 2 rather than that in Figure 1.

More recently, Lockner et al. (1991) studied the failure process in a brittle granite sample deformed in a tri-axial apparatus at a constant confining pressure (50 MPa). The axial load was controlled to maintain a constant rate of acoustic emission during the experiment. Using the post-failure stress curve (obtained quasi-statically) they computed fracture energy, defined as the energy release rate above the work done at the residual stress level (that they called frictional energy). Also these authors rely on a traction evolution similar to that shown in our Figure 1 (see Figure 4 in Lockner et al., 1991), but they called 'frictional energy' the shaded area labeled heat in our Figure 1. This is different from the definition of frictional work given in our equations 7 and 10. Lockner et al. estimated the total energy release (fracture energy, G, and frictional energy) from the acoustic emission energy release to be of the order $(9 \pm 5)\cdot 10^4$ J/m^2, with local variations up to 50%. According to our calculations discussed in previous sections this should correspond to an estimate of the whole frictional work. The authors suggest that the total energy release is a more appropriate parameter to consider rather than fracture energy and frictional energy.

Although there are large uncertainties affecting the values of fracture energy and heat estimated in the laboratory, we believe that the calculations presented above suggest that the partitioning between fracture energy and heat illustrated in Figure 1 and adopted in numerous experimental and theoretical studies is not corroborated by observational evidence and it might be valid only for very specific stress evolutions.

7. SEISMOLOGICAL ESTIMATES OF BREAKDOWN WORK

Many investigators have attempted to infer dynamic parameter from kinematic slip models on extended faults and to understand the physical processes involved during a fault rupture (Miyatake, 1992; Ide and Takeo, 1997; Day et al., 1998; Tinti et al., 2005, among several others). The evaluation of fracture energy for seismic events relies on the knowledge of the dynamic traction evolution. Tinti et al. (2005) have used a 3-D finite difference code (Andrews, 1999) to calculate the stress time series on the earthquake fault plane. The fault is represented by a surface containing double nodes and the stress is computed through the

fundamental elastodynamic equation (Ide and Takeo, 1997; Day et al., 1998). Each node belonging to the fault plane is forced to move with a prescribed slip velocity time series, which corresponds to imposing the slip velocity as a boundary condition on the fault and determining the stress-change time series everywhere on the fault. This numerical approach does not require specification of any constitutive law relating total dynamic traction to friction. The dynamic traction evolution is a result of the calculations.

Inadequate resolution and the limited frequency bandwidth which characterize inverted kinematic models reduce the ability to infer the real dynamic traction evolution everywhere on the fault plane. Many recent papers have investigated the limitations of using poorly resolved kinematic source models (Guatteri and Spudich, 2000; Piatanesi et al., 2004; Spudich and Guatteri 2004). Tinti et al. (2005) have concluded that the estimates of Wb (or G) from (13a) might be stable despite the poor resolution in the kinematic source models, in agreement with Guatteri and Spudich (2000).

Tinti et al. (2005) have computed the breakdown work on extended faults for several moderate to large earthquakes. Plate 1 illustrates the distribution of breakdown work on the fault plane computed for the 1994 Northridge earthquake; it also shows the traction evolution inferred for several selected fault points. This example reveals that the dynamic traction evolution is quite variable on the fault plane. Plate 2 shows the slip and breakdown work distribution on the fault plane for the 1992 Landers earthquake. Although Tinti et al. (2005) calculated both breakdown and restrengthening work in their paper, here we focus on breakdown work and its spatial distribution. On the average, the kinematic models restrengthen, and this feature might be real. However, the procedure used to retrieve traction evolution as a function of slip is based on the assumption of a source time function having a prescribed finite duration in the kinematic slip models (see Piatanesi et al., 2004). The application of our numerical procedure to numerous earthquakes with different kinematic models and source time functions revealed to us that the inferred restrengthening (see Figure 2 and Plate 1) might be biased by the imposed slip velocity function. In other words, we do not believe that our inferred traction evolutions unambiguously support the existence of an undershoot model.

Tinti et al. (2005) present and discuss several distinct calculations for different earthquakes; for each of them they have computed both the local estimate of breakdown work W_b (J/m^2) as well as the breakdown energy E_b (J), which is a global quantity measuring the

contribution of the whole fault. These authors have proposed scaling laws of either the breakdown work or the breakdown energy with seismic moment (see Plate 3); they found a nearly linear relation between E_b and M_o, while the W_b values depends on M_o through a power law whose slope is equal to 0.59. Thrust, normal and strike slip earthquakes display the same scaling with seismic moment. Rice et al. (2005) have presented a quite exhaustive review of fracture energy estimates for several earthquakes. The breakdown work values estimated by Tinti et al. (2005) agree with those proposed by Rice et al. (2005) (Plate 3b).

7.1. Scaling of breakdown work with local slip

As shown in Plate 2, the numerical results of Tinti et al.(2005) indicate that the spatial distributions on the fault plane of breakdown work (W_b) are strongly correlated with the corresponding slip distributions. High slip patches correspond to high W_b values. The correlation between the distributions of W_b and slip is due primarily to the correlation of D_c with slip, but also secondarily to the correlation of stress drop with total slip. One interesting result emerging from Tinti et al. (2005) is that the local W_b values scale as the square of the slip [$W_b \propto (\Delta u)^2$], as clearly shown in Figure 4. This result is consistent with the theoretical predictions obtained by Rice et al. (2005) for the steady-state propagation of a self-healing slip pulse. In fact, the models used by Tinti et al. (2005) are characterized by slip pulses. Abercrombie and Rice (2005) estimated a quantity they called G', inferred from seismic moment and corner frequency, which is equal to the fracture energy only if the final shear stress on the fault is not very different from the residual frictional stress during the last increment of slip. Under these conditions, these authors found that the fracture energy or the breakdown work is related to slip according to the law: $W_b \propto (\Delta u)^{1.3}$. McGarr et al. (2004) using a crack model suggest that fracture energy is linearly related to slip $W_b \propto (\Delta u)^1$. Both these studies used average values of slip to represent the heterogeneous slip distributions over the fault plane. Tinti et al. (2005) have calculated different averages of breakdown work and have discussed the resulting variability of the average (global) breakdown work. More recently, Chambon et al. (2006), interpreting new results from laboratory experiments, propose that fracture energy scales with total slip following a power law with exponent equal to 0.6 [$W_b \propto (\Delta u)^{0.6}$]. Thus, we conclude that the analytical relation to express the scaling of breakdown work with final slip depends on the assumed crack configuration.

7.2. The dependence of breakdown work on rupture velocity

It is well known that energy release rate depends on rupture velocity (see Freund, 1979; McGarr et al., 2004; Rice et al., 2005; Kanamori and Rivera, this volume; among several others). Therefore, the rupture velocity should affect the inferred scaling of breakdown work with earthquake size (see McGarr et al., 2004; Rice et al., 2005 and Plate 3b). However, the dependence of breakdown work on rupture velocity is quite complex and not easy to be modeled analytically. Rice et al. (2005) propose a general expression for the fracture energy, that we apply here to the breakdown work, relating this quantity to the rupture velocity:

$$W_b = \frac{\mu \Delta u^2}{\pi L} F(v_r) g(\theta), \tag{15}$$

where μ is the rigidity, L is the spatial length of the pulse (i.e., the size of the slipping region), $F(v_r)$ is a function of rupture velocity (v_r, which differs for Mode II and Mode III), and $g(\theta)$ is a function of R/L, where R is the length of the breakdown zone (see Rice et al. 2005 for the definition of parameter θ). The latter term can be also considered a function of the ratio T_b/τ_R, where T_b is the duration of the breakdown process and τ_R is the rise time. This relation has been proposed for a self-healing slip pulse and it is appropriate to interpret the estimates of breakdown work inferred from kinematic source models (see Tinti et al., 2005 for further details). It includes the theoretical scaling of breakdown work with the square of final slip plotted in Figure 4.

McGarr et al. (2004) propose a different scaling relation for fracture energy valid for a crack-like model, which we extend here to breakdown work:

$$W_b = 0.24 \cdot F\left(\frac{v_r}{\beta}\right) f(v_r) \Delta\tau_S \cdot \Delta u \tag{16}$$

where β is the shear wave velocity, and $\Delta\tau_s$ is the static stress drop. This relation predicts a linear scaling between breakdown work and slip, as we have anticipated before (although static stress drop should scale with slip). Both relations (15) and (16) contain factors depending on the rupture velocity. In order to provide an example on how rupture velocity can alter the scaling between breakdown work and earthquake size, we plot in Figure 5 the breakdown work as a function of slip for two kinematic source models of the same earthquake; we show breakdown work inferred for the 1979 Imperial Valley earthquake by using the source models proposed by Hartzell and Heaton (1983) and Archuleta (1984). The

latter model involves a super-shear rupture velocity. It is evident that while the inferred scaling between W_b and slip fits the local values retrieved for the Hartzell and Heaton model, the behavior obtained for the Archuleta's model is much more complex.

It is important to mention that, because of the limited frequency bandwidth currently adopted to invert seismograms, the inferred slip models do not contain information on the actual rupture velocity variations during the dynamic rupture propagation. This may affect the inferred local traction evolutions and therefore bias the estimation of breakdown work at specific points on the fault plane. We may face this problem by recognizing that fluctuations of the breakdown work estimates are likely to occur. Moreover, we rely on some average values of W_b estimated on the whole fault or on particular patches of the rupture plane. Rice et al. (2005) suggest that seismological estimates of fracture energy might be only a fraction of the real energy absorbed during the dynamic rupture propagation. If excessive energy is removed from the kinematic rupture models by low-pass filtering of the seismograms, Spudich and Guatteri (2004) showed that breakdown work can be overestimated. However, we believe that the inferred scaling relation with earthquake size might still be representative of the earthquake energy scaling.

8. THE PARTITION BETWEEN SURFACE ENERGY AND HEAT

In this study we have defined the macroscopic frictional work (eq. 11a) and we have shown that it contains surface energy and heat (eq.3). Because absolute stress on the fault plane is unknown (unless for peculiar conditions, Spudich et al. 1998) we can only measure the frictional work over some minimum or residual stress value. This work corresponds to our breakdown work, and in this section we compare our breakdown work estimates with geological estimates of surface energy to provide some observational evidence constraining the relative proportions of surface energy and heat (Tinti et al. 2005).

Plate 4 shows the breakdown work estimated from a variety of kinematic slip models of earthquakes by Tinti et al. [2005, their Table 2] as a function of seismic moment and compares these values to geological estimates of surface energy.

Open squares are the estimates for the part of the fault having slip exceeding 20% of the average slip in the event (this excludes the poorly resolved low slip zones), and open circles are estimates for the earthquake's "asperities," specifically the parts of the fault having slip

greater than 70% of the maximum slip anywhere on the fault. Solid black squares show the range of surface energies estimated by Wilson et al. (2005) for the October 1997 Bosman fault earthquake in the Hartebeestfontein mine, South Africa, and for a typical paleo-earthquake on the San Andreas fault at Tejon Pass, California. Solid triangles show the range of surface energy estimated for a typical paleo-earthquake on the Punchbowl fault in California, which was a prior plate boundary fault. (We have adjusted the Bosman earthquake's magnitude to 4.8 from Wilson's 3.7 based on slip scaling in McGarr and Fletcher (2003), and we assigned a magnitude of 7.5 to the California paleo-earthquakes). The solid circle shows the $8 \cdot 10^6$ J/m^2 estimate of heat production made by Matsumoto et al. (2001) based on electron spin resonance measurement of partial defect annealing in quartz obtained from a borehole at 389 m depth on a branch of the Nojima fault near Toshima, Awaji Island, Japan, that probably slipped during the 1995 Kobe (Hyogo-ken Nanbu) earthquake.

Before addressing the obvious differences between the seismological and geological energy estimates, we must first comment on the geological estimates. The geologic settings of the four measurements are quite different. The Bosman earthquake ruptured previously intact quartzite, creating the Bosman fault, which was characterized by 10-30 subparallel ~1-mm-wide fractures containing gouge. Wilson et al. (2005) obtained their surface energy estimate by measuring the particle size distribution (PSD) of the gouge in the fault zone, which was accessible through a mine shaft. At Tejon Pass they measured the PSD and surface energy of the pervasively pulverized granite in a 70-100-m-wide zone on the San Andreas exposed at the surface. This Tejon Pass measurement is less accurate than the Bosman measurement because Wilson et al. had no direct measurement of the width of the powder zone created by a single earthquake; they divided the 100-m-wide zone by 10000 earthquakes to estimate that 10 mm of gouge was created in each earthquake. Chester et al. (2005) measured the PSD and surface energy of the gouge and microfractures across the entire damage zone around the Punchbowl fault, which, unlike the San Andreas at Tejon Pass, contains a 1-mm-wide principal slip surface on which almost all of the slip occurred. The Nojima fault at Ogura consists of several splays. The Nojima fault in Matsumoto's borehole had a 100-mm-wide gouge zone separating granite and sedimentary rocks, and the gouge zone contained a single, shiny slickensided surface.

Because the geologic settings of the Bosman, Tejon Pass, and Punchbowl surface energy measurements are different, we believe that they must be applied to differing regions

of faults. It is probably most appropriate to compare the Tejon Pass and Bosman measurements to geometrically complicated parts of faults. Because the Tejon Pass pulverized zone is 70-100 m wide, it probably represents an exhumed fault jog [J. Chester, personal communication, 2004] where the evolving fault geometry over time caused frequent fresh fracture during earthquakes and a broad powder zone, rather than repeated comminution of the same gouge zone over thousands of earthquakes as in the Punchbowl fault. This is a possible explanation for the similarity of the Tejon Pass PSD to the Bosman PSD reported by Wilson et al. (2005) If this explanation is true, the similarity of the Tejon Pass and Bosman surface energies is initially surprising given the much larger slip per event expected for the San Andreas compared to the Bosman, but Power et al. (1988) report that most gouge is generated during the initial part of slip (first 15 mm in their experiments). In contrast, the Punchbowl surface energy is more appropriately compared to straighter sections of faults. However, Reches and Dewers (2005) have appealed to another mechanism, dynamic pulverization by extreme volumetric stress changes at the crack tip, as the cause of the similar PSDs.

Evidence in Plate 4 suggests that surface energy is a small fraction (1-10 %) of breakdown work most places on major faults except at geometrically complicated regions like fault jogs, and possibly even there too. The Punchbowl surface energy is considerably smaller than breakdown work measured for all the events having moment exceeding 10^{18} Nm. Even the Tejon Pass surface energy is considerably less than breakdown work for the 1992 Landers earthquake. Interestingly, the heat generation measured by Matsumoto et al. (2001) for the 1995 Kobe earthquake is comparable to that event's breakdown work, but the heat measurement comes from about 400 m depth, whereas the breakdown work is observed much deeper, so the significance of this observation is unclear.

9. SUMMARY

In this study we have defined the macroscopic frictional work as the integral of the shear traction as a function of slip; this means that the area below the slip weakening curve defines the amount of frictional work absorbed during faulting. This definition is consistent with the earthquake energy budget derived from an elastic body containing a fault surface. The surface energy absorbed during faulting is part of the macroscopic frictional work and therefore comprises some fraction of the area below the slip weakening curve. Because for

realistic fault zone models the stress is not singular at the crack tip, the effective surface energy γ_{eff}, often included in the earthquake energy balance as well as in different definitions of the radiated seismic energy, is zero. Therefore, we conclude that all the mechanical work absorbed on the fault plane is the macroscopic frictional work. Moreover, because the absolute stress level on the fault is unknown except in special cases (e.g. Spudich et al., 1998), the only measurable quantity is the breakdown work, which depends on the area above the minimum value of dynamic traction.

Breakdown work itself is also comprised of a mixture of surface energy and heat (intended as a dissipative term as defined by KD88). The comparison between geological estimates of surface energy and the breakdown work estimated for recent earthquakes by Tinti et al. (2005) reveals that surface energy is 1 - 10% of the average breakdown work. We have also pointed out that in a realistic fault zone model the transition between heat and surface energy can lie everywhere below the slip weakening curve, as we have drawn in the schematic sketch of Figure 2.

Acknowledgements

We thank Stefan Nielsen, Eiichi Fukuyama, Giulio Di Toro and Judith Chester for useful discussions. We thank Art McGarr, Eiichi Fukuyama and an anonymous reviewer for their helpful comments which allowed us to improve the manuscript.

References

Abercrombie, R.E., and J.R. Rice (2005), Can observations of earthquake scaling constrain slip weakening?, *Geophys. J. Int., 162*, 406-424.

Andrews, D J. (2002), A fault constitutive relation accounting for thermal pressurization of pore fluid, *J. Geophys. Res., 107*, 2363, doi:10.1029/2002JB001942.

Andrews, D.J. (1976a), Rupture propagation with finite stress in antiplane strain, *J. Geophys. Res, 81*, 3575 – 3582.

Andrews, D.J. (1976b), Rupture velocity of plane strain shear cracks*, J. Geophys. Res., 81*, 5679 – 5687.

Andrews, D.J. (1999), Test of two methods for faulting in finite-difference calculations, *Bull. Seismol. Soc. Am.*, *89*, 931-937.

Andrews, D.J. (2005), Rupture dynamics with energy loss outside the slip zone*, J. Geophys. Res., 110*, 1307, doi: 10.1029/2004JB003191.

Archuleta, R.J. (1984), A faulting model for the 1979 Imperial Valley earthquake, *J. Geophys. Res., 89*, 4559-4585.

Barenblatt, G.I. (1959), The formation of equilibrium cracks during brittle fracture. General ideas and hypotheses. Axially-symmetric cracks*, J. Appl. Math. Mech., 23*, 1273 - 1282.

Bizzarri, A., and M. Cocco (2006a), A thermal pressurization model for the spontaneous dynamic rupture propagation on a 3-D fault: Part I – Methodological approach, *J. Geophys. Res.*, *111*, 5303, doi:10.1029/2005JB003862

Bizzarri, A., and M. Cocco (2006b), A thermal pressurization model for the spontaneous dynamic rupture propagation on a 3-D fault: Part II – Traction evolution and dynamic parameters, *J. Geophys. Res.*, *111*, 5304, doi:10.1029/2005JB003864.

Chambon, G., J. Shmittbuhl, and A. Corfdir (2006), Frictional response of a thick gouge sample: I Mechanical measurements and microstructures, *J. Geophys. Res., 111*, 9308, doi:10.1029/2003JB002731.

Chester, F.M., J.P. Evans, and R.L. Biegel (1993), Internal structure and weakening mechanisms of the San Andreas fault, *J. Geophys. Res., 98*, 771-786**.**

Chester, J.S., F.M. Chester, and A.K. Kronenberg (2005), Fracture surface energy of the Punchbowl fault, San Andreas system, *Nature, 437*, 133-136.

Day, S.M., G. Yu and D.J. Wald (1998), Dynamic stress changes during earthquake rupture, *Bull. Seismol. Soc. Am.*,*88*, 512-522.

Di Toro, G., S. Nielsen, and G. Pennacchioni (2005), Earthquake rupture dynamics frozen in exhumed ancient faults, *Nature*, *436*, 1009-1012.

Fialko Y.A. (2004), Temperature fields generated by the elastodynamic propagation of shear cracks in the Earth, *J. Geophys. Res.*, *109*, 1303, doi: 10.1029 / 2003JB002497.

Freund, L.B. (1979), The mechanics of dynamic shear crack propagation, *J. Geophys. Res.*, *84*, 2199-2209.

Fukuyama, E. (2005), Radiation energy measured at earthquake source, *Geophys. Res. Lett.*, *32*, L13308, doi:10.1029/2005GL022698.

Griffith, A.A. (1920), The phenomenon of rupture and flow in solids, *Phil. Trans. Roy. Soc. London, Ser. A, 222*, 163-198.

Guatteri, M. and P. Spudich (2000), What can strong-motion data tell us about slip-weakening fault-friction laws?, *Bull. Seismol. Soc. Am.*, *90*, 98-116.

Hartzell, S.H. and T.H. Heaton (1983), Inversion of strong ground motion and teleseismic waveform data for the fault rupture history of the 1979 Imperial Valley, California, earthquake, *Bull. Seismol. Soc. Am.*, *73*, 1553-1583.

Hernandez, B., F. Cotton, and M. Campillo (1999), Contribution of radar interferometry to a two-step inversion of the kinematic process of the 1992 Landers earthquake, *J. Geophys. Res.*, *104*, 13083-13099.

Ida, Y. (1972), Cohesive force across the tip of a longitudinal–shear crack and Griffith's specific surface energy, *J. Geophys. Res., 77*, 3796-3805.

Ide, S. and M. Takeo (1997), Determination of constitutive relations of fault slip based on seismic wave analysis, *J. Geophys. Res.*, *102*, 27379-27391.

Irwin, G. R. (1960), Fracture mechanics, in *Structural Mechanics*, edited by J.N. Goodier and N.J. Hoff, pp. 557-591, Pergamon Press, Elmsford, NY.

Kanamori, H., and T.H., Heaton (2000), Microscopic and macroscopic physics of earthquakes, in *Geocomplexity and the Physics of Earthquakes, Geophys. Monogr. Ser.,* vol. 120, edited by J. Rundle, et al., pp. 147-163, AGU, Washington, D.C.

Kanamori, H., and L. Rivera (2006), Energy partitioning during an earthquake, in this Monograph Volume.

Kato, A., M. Ohnaka, and H. Mochizuki (2003), Constitutive properties for the shear failure of intact granite in seismogenic environments, *J. Geophys. Res.*, *108*, doi:10.1029/2001JB000791.

Kostrov, B.V. (1974), Self-similar problems of propagation of shear cracks, *J. Appl. Math. Mech.*, *28*, 1077-1087.

Kostrov, B.V., and S. Das (1988), *Principles of Earthquake Source Mechanics*, 286 pp., Cambridge Univ. Press, New York.

Li, V.C. (1987), Mechanics of shear rupture applied to earthquake zones, in *Fracture Mechanics of Rock*, edited by B. Atkinson, pp. 351-428, Academic Press, London.

Lockner, D.A., J.D. Byerlee., V. Kuksenko, A. Ponomarev, and A. Sidorin (1991), Quasi-static fault growth and shear fracture energy in granite, *Nature*, *350*, 39-42.

Lockner, D.A., and P.G. Okubo (1983), Measurements of frictional heating in granite, *J. Geophys. Res., 88,* 4313-4320.

Matsumoto, H., C. Yamanaka, and M. Ikeya (2001), ESR analysis of the Nojima fault gouge, Japan, from the DPRI 500 m borehole, *The Island Arc, 10*, 479-485.

McGarr, A. (1994), Some comparisons between mining-induced and laboratory earthquakes, *Pure Appl. Geophys.*, *142*, 467- 489.

McGarr, A., J.B. Fletcher, and N.M. Beeler (2004), Attempting to bridge the gap between laboratory and seismic estimates of fracture energy, *Geophys. Res. Lett.*, *31*, L14606, doi:10.1029/2004GL020091.

McGarr, A., and J.B. Fletcher (2003), Maximum slip in earthquake fault zones, apparent stress, and stick-slip friction, *Bull. Seismol. Soc. Am., 93*, 2355-2362.

Mikumo, T., K.B. Olsen, E. Fukuyama, and Y. Yagi (2003), Stress-breakdown time and slip-weakening distance inferred from slip-velocity functions on earthquake faults, *Bull. Seismol. Soc. Am., 93*, 264-282.

Miyatake, T. (1992), Reconstruction of dynamic rupture process of an earthquake with constraints of kinematic parameters, *Geophys. Res. Lett.*, *19*, 349-352.

Moore, D.E., and D.A. Lockner (1995), The role of microcracking in shear-fracture propagation in granite, *J. Struct. Geol.*, *17*, 95-114.

Ohnaka, M. (1996), Nonuniformity of the constitutive law parameters for shear rupture and quasistatic nucleation to dynamic rupture: A physical model of earthquake generation processes, *Proc. Nat. Acad. Sci. USA*, *93*, 3795-3802.

Ohnaka, M., M. Akatsu, H. Mochizuki, A. Odera, F. Tagashira, and Y. Yamamoto (1997), A constitutive law for the shear failure of rock under lithospheric conditions, *Tectonophysics*, *277*, 1-27.

Ohnaka, M. (2003), Constitutive scaling law and a unified comprehension for frictional slip failure, shear fracture of intact rock, and earthquake rupture, *J. Geophys. Res.*, *108*, 2080, doi:10.1029/2002JB000123.

Okubo, P.G., and J. H. Dieterich (1984), Effects of physical fault properties on frictional instabilities produced on simulated faults, *J. Geophys. Res.*, *89*, 5817-5827.

Palmer, A.C., and J.R. Rice (1973), The growth of slip surfaces in the progressive failure of over- consolidated clay, *Proc. R. Soc. London Ser. A, 332*, 527 – 548

Parton, V.Z., and E.M. Morozov (1974), *Elastic-Plastic Fracture Mechanics*, 427 pp., Mir Publishers Moscow.

Piatanesi, A., E. Tinti, M. Cocco and E. Fukuyama (2004), The dependence of traction evolution on the earthquake source time function adopted in kinematic rupture models, *Geophys. Res. Lett., 31,* doi:10.1029/2003GL019225.

Power, W.L., T.E. Tullis, and J.D. Weeks (1988), Roughness and wear during brittle faulting, *J. Geophys. Res, 93,* 15268-15278.

Reches, Z., and T.A. Dewers (2005), Gouge formation by dynamic pulverization during earthquake rupture, *Earth Plan. Sci. Let*., *235*, 361-374.

Rice, J.R., and M., Cocco (2006), Seismic fault rheology and earthquake dynamics, in *Dahlem Workshop on The Dynamics of Fault Zones*, edited by M. R. Handy, MIT Press, Cambridge, Mass., in press.

Rice, J.R., C.G. Sammis, and R. Parsons (2005), Off-fault secondary failure induced by a dynamic slip pulse, *Bull Seismol. Soc. Am.*, *95*, 109-134.

Rivera, L., and H. Kanamori (2005), Representations of the radiated energy in earthquakes, *Geophys. J. Int.*, *162*, 148-155.

Rudnicki, J.W. and L.B. Freund (1981), On energy radiation from seismic sources, *Bull. Seismol. Soc. Am., 71*, 583-595.

Rummel, F., H. J., Alheid, and C. Frohn (1978), Dilatancy and fracture induced velocity changes in rock and their relation to frictional sliding, *Pure Appl. Geophys., 116,* 743-764.

Scholz, C. H. (1990), *The Mechanics of Earthquake and Faulting*, 439 pp., Cambridge Univ. Press, Cambridge.

Shimamoto, T. and A. Tsutsumi (1994), A new rotary-shear high-velocity frictional testing machine: Its basic design and scope of research, *J. Struct. Geol.*, *39*, 65-78

Sibson, R.H. (1973), Interaction between temperature and pore-fluid pressure during earthquake faulting – A mechanism for partial or total stress relief, *Nature*, *243*, 66-68.

Sibson, R.H. (2003), Thickness of seismic slip zone, *Bull. Seismol. Soc. Am.*, *93*, 1169-1178.

Spudich, P., M. Guatteri, K. Otsuki,and J. Minagawa (1998), Use of fault striations and dislocation models to infer tectonic shear stress during the 1995 Hyogo-ken Nanbu (Kobe) earthquake, *Bull. Seismol. Soc. Am., 88*, 413-427.

Spudich, P., and M. Guatteri (2004), The effect of bandwidth limitations on the inference of earthquake slip-weakening distance from seismograms, *Bull. Seismol. Soc. Am., 94*, 2028-2036.

Tinti, E., P. Spudich, and M. Cocco (2005), Earthquake fracture energy inferred from kinematic rupture models on extended faults, *J. Geophys. Res.*, *110,* 12303, doi: 10.1029/2005JB003644.

Wald, D.J., and T.H. Heaton (1994), Spatial and temporal distribution of slip for the 1992 Landers, California, earthquake, *Bull. Seismol. Soc. Am., 84,* 668-691.

Wald D.J., T.H Heaton, and K.W. Hudnut (1996), The slip history of the 1994 Northridge, California, earthquake determined from strong-motion, teleseismic, GPS, and leveling data, *Bull. Seismol. Soc. Am., 86*, S49-S70 Part B Suppl.

Wilson, B., T. Dewers, Z. Reches, and J. Brune (2005), Particle size and energetics of gouge from earthquake rupture zonessss, *Nature, 434*, 749-752.

Wong, T.-f. (1982), Effects of temperature and pressure on failure and post-failure behavior of Westerly granite, *Mech Mater.*, *1,* 3-17.

Table 1. List of earthquakes used to infer breakdown work and shown in Figure 9.

Code	Quake	Model
MHB	1984 Morgan Hill	Beroza and Spudich (1988)
C33	1997 Colfiorito 0033	Hernandez et al.(2004)
C09	1997 Colfiorito 0940	Hernandez et al.(2004)
COc	1997 Colfiorito-Oct	Hernandez et al.(2004)
IVA	1979 Imperial Valley	Archuleta (1984)
IVH	1979 Imperial Valley	Hartzell and Heaton (1994)
ToY	2000 Western Tottori	Y.Yagi's model reported by Mikumo et al. (2003)
ToS	2000 Western Tottori	written communication, H. Sekiguchi, 2002
TP1	2000 Western Tottori	A. Piatanesi's unpublished data
TP2	2000 Western Tottori	A. Piatanesi's unpublished data
KoW	1995 Kobe	Wald (1996)
LWH	1992 Landers	Wald and Heaton (1994)
LHe	1992 Landers	Hernandez et al (1999)
NoW	1994 Northridge	Wald et al. (1996)

Figure

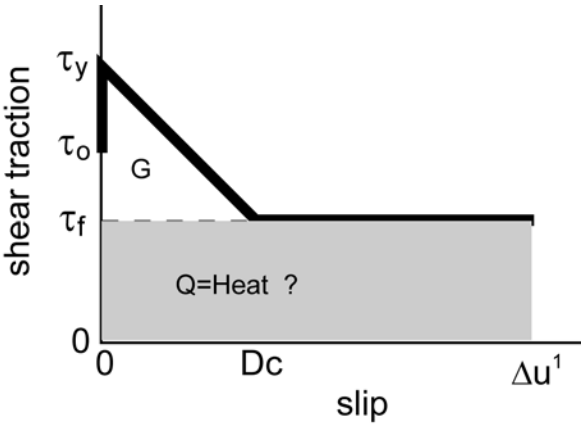

Figure 1. Slip weakening model. D_c is the slip weakening distance, Δu^1 is the final slip and G is the fracture energy. The work below the residual friction level is often assumed to be heat, but there is no justification for this assumption.

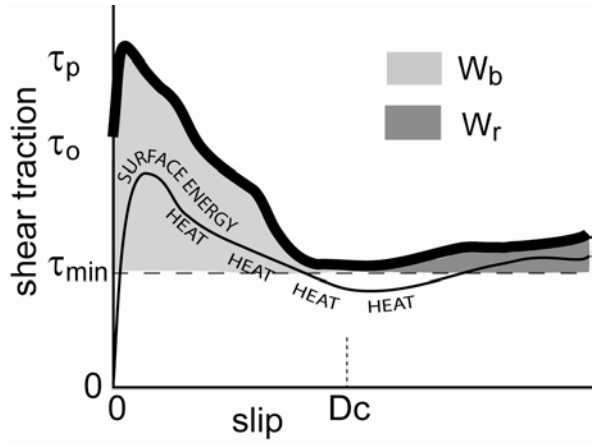

Figure 2. Idealized sketch showing traction as a function of slip and the partitioning of frictional work between surface energy and heat.

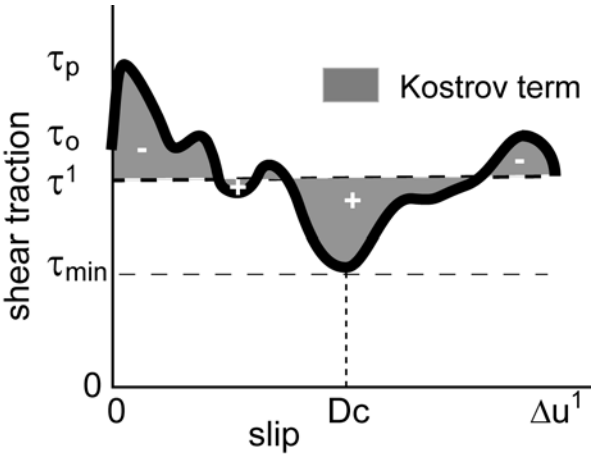

Figure 3. Sketch illustrating the contributions to the Kostrov term defined in (12).

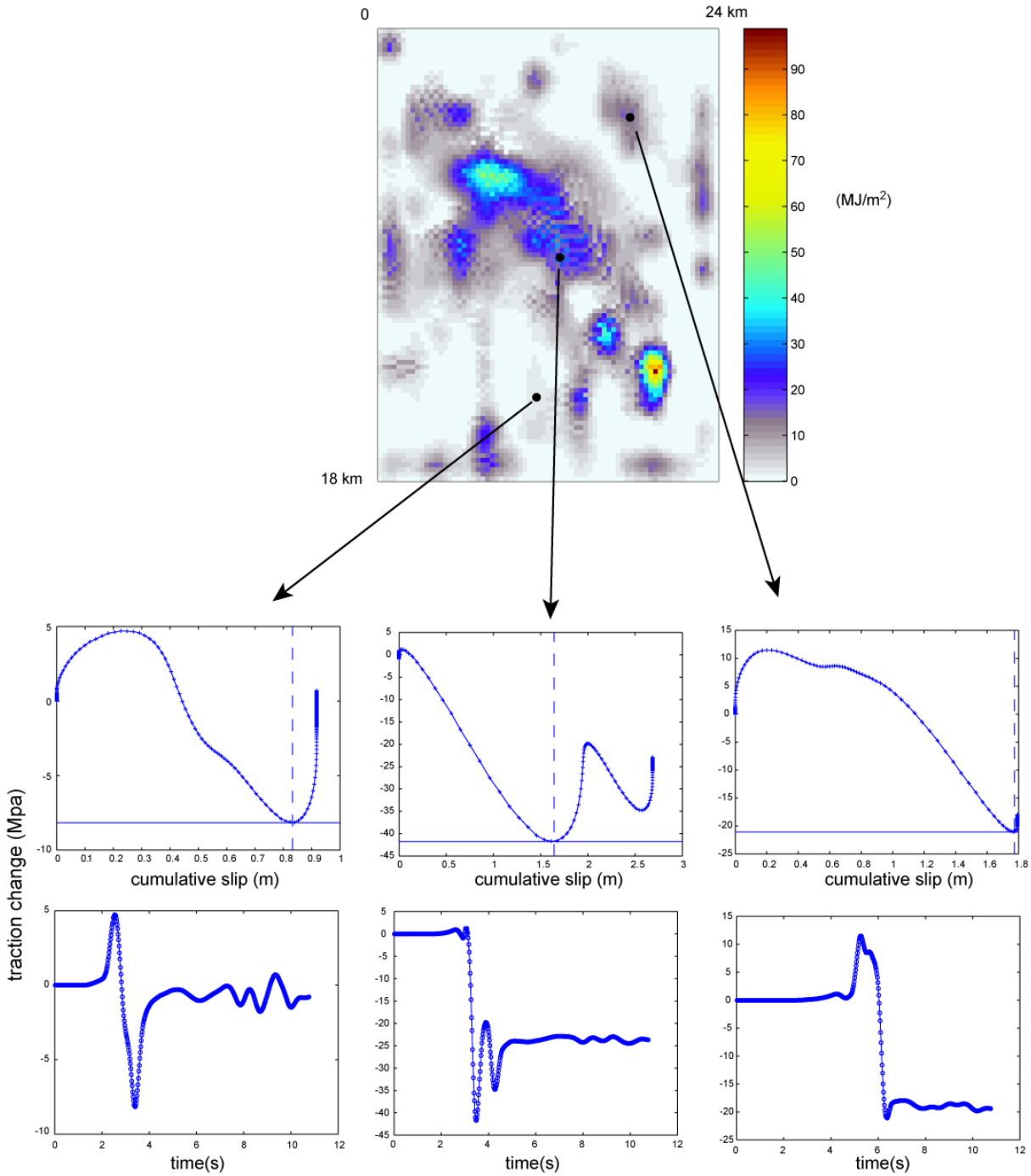

Plate 1. Breakdown work distribution inferred by Tinti et al. (2005) for the 1994 Northridge earthquake (top plot). The middle row shows the traction versus slip evolution and bottom row shows the traction versus time evolution for several target points on the fault plane indicated by the black dots.

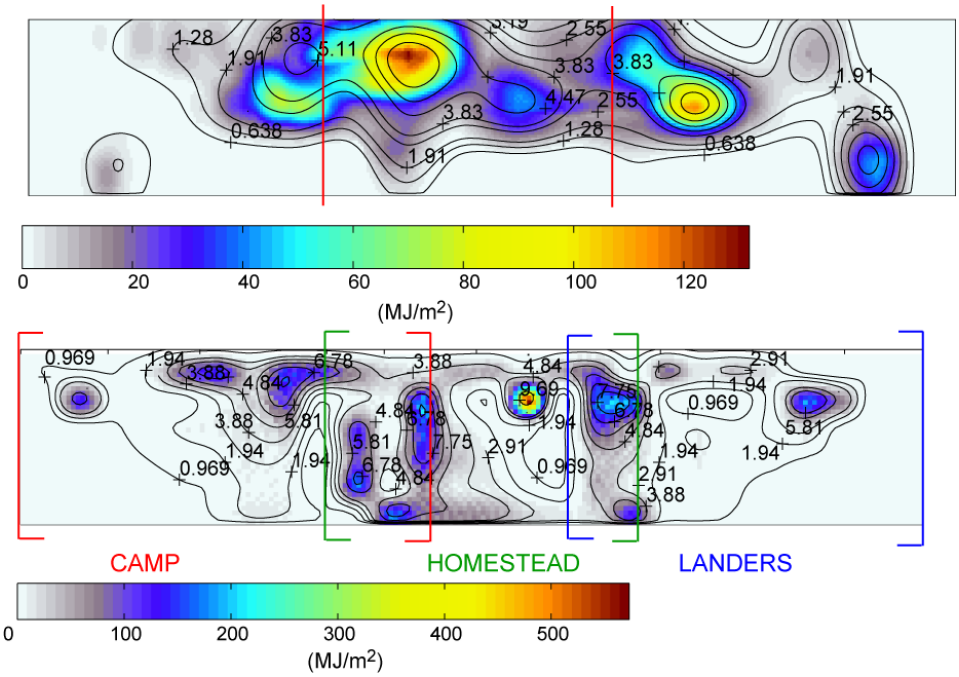

Plate 2. Breakdown work distribution inferred by Tinti et al. (2005) for two kinematic models of the 1992 Landers earthquake: the Hernandez et al. (1999) [upper panel] and Wald and Heaton (1994) [bottom panel]. The color bar unit is MJ/m^2. Contour lines show the slip distribution and numbers indicate slip values. Matching color brackets indicate ends of fault planes in the Wald and Heaton model of Landers.

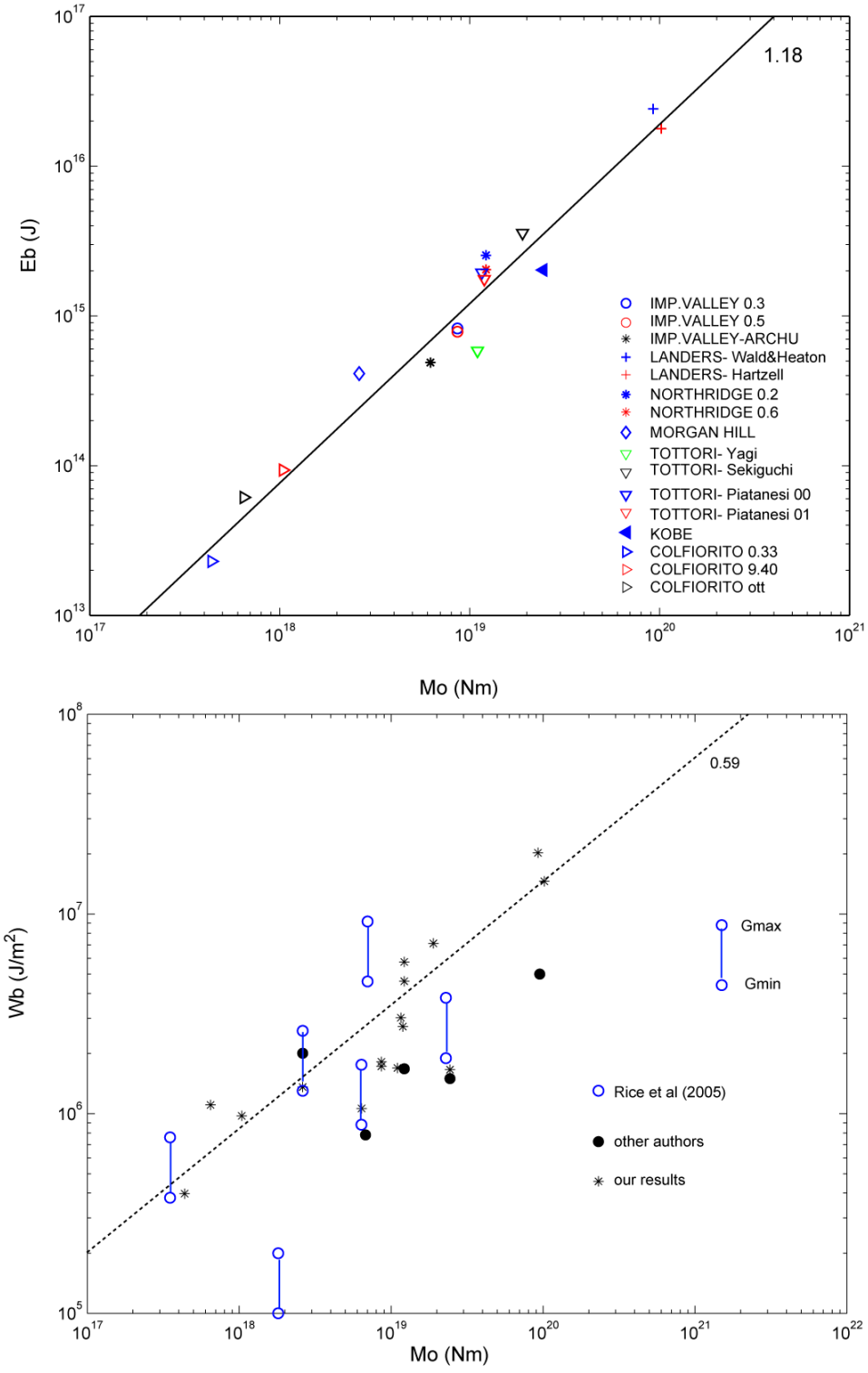

Plate 3. Breakdown energy (upper panel) and breakdown work densities (lower panel) averaged over the whole fault versus seismic moment for all the earthquake modeled by Tinti et al. (2005) shown by asterisks and estimates reported by Rice et al. (2005) and other authors. Symbols for various earthquakes are listed on the legend.

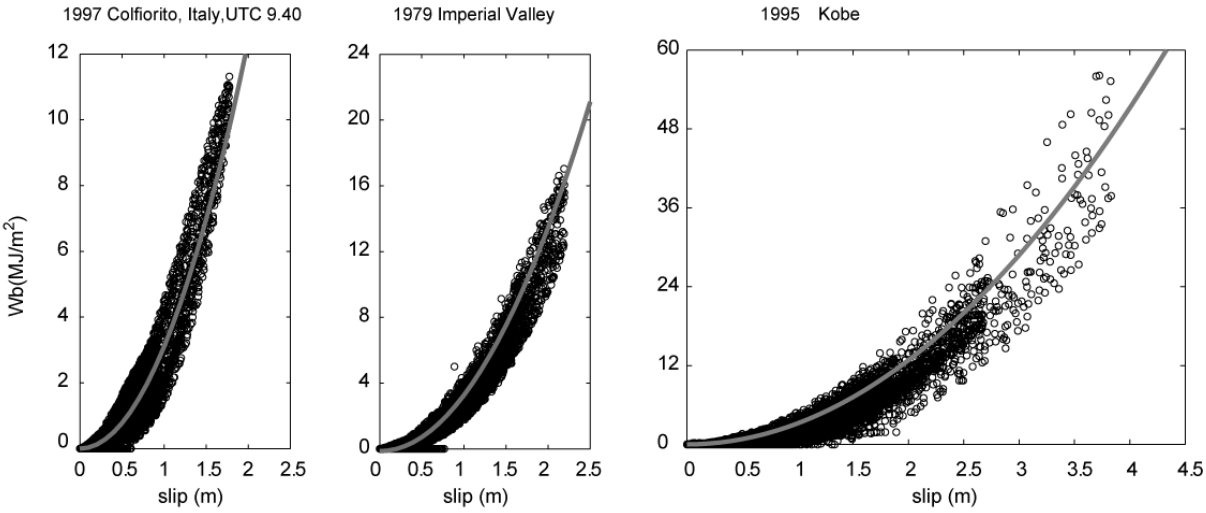

Figure 4. Breakdown work density versus total slip for each point on fault of the 1997 Colfiorito, 1979 Imperial Valley and 1995 Kobe earthquake models. The superimposed grey curve depicts a quadratic function.

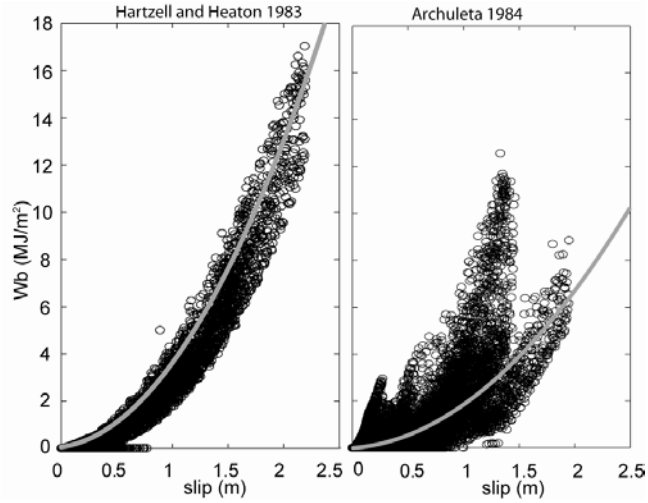

Figure 5. Breakdown work density versus total slip for each point on fault of the 1979 Imperial Valley earthquake models proposed by Hartzell and Heaton (1983) and Archuleta (1994). The superposed grey curve depicts a quadratic function.

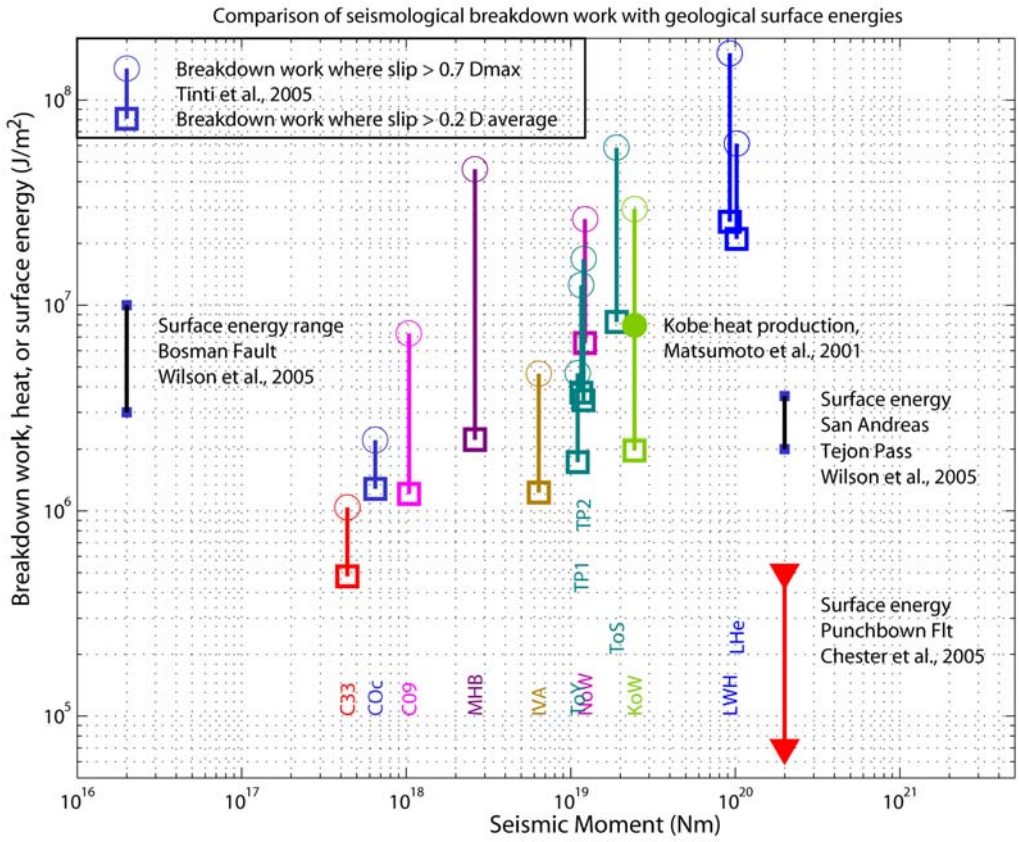

Plate 4. Comparison of seismologically estimated breakdown work [Tinti et al., 2005], geologically estimated surface energy [Wilson et al., 2005; Chester et al., 2005], and geologically estimated heat production [Matsumoto et al., 2001] for several earthquakes. Open circles and squares show breakdown work averaged over portions of the faults having slip exceeding threshold amounts (see legend) in slip models indicated by three-letter codes **(Table 1)**. Each earthquake has a different color. Solid squares and triangles show surface energy estimated by direct observation in fault zone materials. Solid circle is heat production in the 1995 Kobe earthquake estimated from electron spin resonance measurements. (Note added in proof: Measurements by Wilson et al. (2005) have been called into question and are probably too high.)